# Nucleotide and $Mg^{2+}$ Dependency of the Thermal Denaturation of Mitochondrial $F_1$-ATPase

Joaquim Villaverde,* Josep Cladera,* Aloysius Hartog,# Jan Berden,# Esteve Padrós,* and Mireia Duñach*
*Unitat de Biofísica, Departament de Bioquímica i Biologia Molecular, Facultat de Medicina, Universitat Autònoma de Barcelona, 08193 Bellaterra, Spain, and #E. C. Slater Instituut, Universiteit van Amsterdam, 1018 TV Amsterdam, the Netherlands

ABSTRACT The influence of adenine nucleotides and $Mg^{2+}$ on the thermal denaturation of mitochondrial $F_1$-ATPase ($MF_1$) was analyzed. Differential scanning calorimetry in combination with ATPase activity experiments revealed the thermal unfolding of $MF_1$ as an irreversible and kinetically controlled process. Three significant elements were analyzed during the thermal denaturation process: the endothermic calorimetric transition, the loss of ATP hydrolysis activity, and the release of tightly bound nucleotides. All three processes occur in the same temperature range, over a wide variety of conditions. The purified $F_1$-ATPase, which contains three tightly bound nucleotides, denatures at a transition temperature ($T_m$) of 55°C. The nucleotide and $Mg^{2+}$ content of $MF_1$ strongly influence the thermal denaturation process. First, further binding of nucleotides and/or $Mg^{2+}$ to $MF_1$ increases the thermal denaturation temperature, whereas the thermal stability of the enzyme is decreased upon removal of the endogenous nucleotides. Second, the stabilizing effect induced by nucleotides is smaller after hydrolysis of ATP (i.e., in the presence of ADP · $Mg^{2+}$) than under nonhydrolytical conditions (i.e., absence of $Mg^{2+}$ or using the nonhydrolyzable analog 5′-adenylyl-imidodiphosphate). Third, whereas the thermal denaturation of $MF_1$ fully loaded with nucleotides follows an apparent two-state kinetic process, denaturation of $MF_1$ with a low nucleotide content follows more complex kinetics. Nucleotide content is therefore an important factor in determining the thermal stability of the $MF_1$ complex, probably by strengthening existing intersubunit interactions or by establishing new ones.

## INTRODUCTION

The ATP synthases ($F_0F_1$ type) are found in the membranes of bacteria, chloroplasts, and mitochondria. They are the final coupling factor between an electrochemical proton gradient and ATP synthesis during oxidative or photosynthetic phosphorylation. The structure and catalytic mechanism of the enzyme have been exhaustively reviewed (Boyer, 1993; Weber and Senior, 1997). In all organisms the ATP synthase is composed of a transmembrane $F_0$ portion, which acts as a proton channel, linked to an hydrophilic $F_1$ portion, where nucleotide binding and ATP synthesis occur. The $F_1$ moiety can be isolated as a soluble complex, containing five subunits in a stoichiometry of $\alpha_3\beta_3\gamma\delta\epsilon$, with a molecular mass of 370,000 Da. This complex has only ATPase activity, the reverse of the physiological function. An important step toward our understanding of the enzyme has been the publication of the high-resolution structure of beef heart $F_1$ (Abrahams et al., 1994), crystallized in a buffer containing the nucleotides ADP and 5′-adenylyl-imidodiphosphate (AMPPNP). The overall structure shows $\alpha$ and $\beta$ subunits with a similar folding, alternatively arranged in a hexamer around the central $\gamma$ subunit. Two important features regarding the nucleotide binding sites, reported in Abrahams' work, are their location within the protein and their asymmetry. As expected from many photolabeling experiments, the nucleotides are indeed found at the interfaces between the $\alpha$ and $\beta$ subunits; the catalytic sites are mainly formed by the $\beta$ subunits, and conversely, the noncatalytic sites are formed mainly with the $\alpha$ subunits. The nucleotide filling pattern as well as the precise orientation of subunits were found to be asymmetrical in this structure. Thus two $\beta$ subunits contained bound nucleotide (ADP or AMPPNP), whereas the binding site on the third $\beta$ subunit was empty. The three $\beta$ subunit conformations were different and were designed as tight, loose, and open, respectively. Moreover, the single $\gamma$ subunit had asymmetrical contacts with the $\beta$ subunits. These differences in conformation and in nucleotide content have been related in the paper of Abrahams et al. (1994) to the binding-change mechanism of catalysis proposed by Boyer (1993). In this mechanism $\beta$ subunits go sequentially through three different conformations: tight, loose, and open, which might be similar to the three found in the crystal structure. Abrahams et al. (1994) suggested that during catalysis, as each $\beta$ subunits goes through these three states, the $\alpha_3\beta_3$ complex may rotate around the central $\gamma$ subunit. This suggestion, although not in line with several data on the properties of the nucleotide binding sites of the mitochondrial enzyme (Berden et al., 1991), has recently been corroborated through the use of different techniques (Junge et al., 1997). The authors presented a direct observation of a unidirectional rotation of the $\gamma$ subunit around the immobilized $\alpha_3\beta_3$ complex during ATP hydrolysis.

ATP hydrolysis by $F_1$ ATPase displays complex features. From the first studies on the mechanism of catalysis, cooperativity between catalytic sites was evident, because binding of the substrate to at least two sites is needed for rapid catalysis. In addition, two apparent values of $K_m$ for ATP are obtained under conditions of rapid catalysis (Grubmeyer

*Received for publication 20 January 1998 and in final form 29 June 1998.*
Address reprint requests to Dr. Mireia Duñach, Unitat de Biofísica, Facultat de Medicina, Universitat Autònoma de Barcelona, 08193 Bellaterra, Spain. Tel.: +34-93-581-1870; Fax: +34-93-581-1907; E-mail: m.dunach@cc.uab.es.

0006-3495/98/10/1980/09 $2.00

and Penefsky, 1981; Cross et al., 1982). In other words, binding to a second site accelerates the release of products from the first site (Gresser et al., 1982; Nalin and Cross, 1982), and nucleotide binding at an additional site, catalytic or noncatalytic, modulates the properties of the catalytic sites (Milgrom and Cross, 1993). Involvement of a noncatalytic site in the apparent negative cooperativity of binding has been shown (Edel et al., 1993; Jault and Allison, 1993, 1994). The modulating role of noncatalytic sites is supported by the finding that the nucleotide-depleted enzyme shows only one $K_m$ value for ATP hydrolysis (Reynafarje and Pedersen, 1996). On the other hand, the role of $Mg^{2+}$ is also important. The presence of $Mg^{2+}$ induces the asymmetry of the catalytic sites of *Escherichia coli* $F_1$ (Senior et al., 1995; Weber and Senior, 1996). They showed that the catalytic binding sites have the same affinity for ATP in the absence of $Mg^{2+}$, but display different affinities for ATP · $Mg^{2+}$. Furthermore, in the presence of ATP and $Mg^{2+}$, the enzyme evolves after catalysis to an inhibited state, containing tightly bound ADP · $Mg^{2+}$ at a catalytic site (Murataliev, 1992; Murataliev and Boyer, 1994).

These observations suggest that several conformational changes should occur in $F_1$ upon nucleotide or $Mg^{2+}$ binding. These changes preserve the main arrangement (alternating $\alpha_3\beta_3$ complex around the central $\gamma$ subunit), but cause intra- and intersubunit movements, which are important for catalysis (Futai et al., 1995).

In this study the thermal stability of beef heart $F_1$ was analyzed under conditions of different nucleotide and $Mg^{2+}$ content, including the conditions used in the above-mentioned crystallization studies. Differential scanning microcalorimetry (DSC) and inactivation studies provide information on the thermal unfolding process of the proteins, and may allow conclusions to be drawn on intersubunit and subunit-ligand interactions (Haltia and Freire, 1995; Sánchez-Ruiz, 1992, 1995). In this study, we report data demonstrating a strong influence of the nucleotide occupancy of the enzyme on the temperature of denaturation, as well as on the denaturation process itself, reflecting the different functional states of the enzyme. In this context, $F_1$ ATPase from chloroplast was previously studied by Wang et al. (1993) by DSC. Their work relies on the nucleotide filling pattern described by Shapiro et al. (1991), and in all experiments $Mg^{2+}$ was present. The interpretation of the results of Wang et al. (1993) was hampered by the fact that $CF_1$ is subjected to two types of inhibition not present in the mitochondrial $F_1$-ATPase ($MF_1$) preparations: $CF_1$ has to be reduced to be fully active, and the $\epsilon$ subunit acts as an inhibitor of $CF_1$. The functional and structural differences between $CF_1$ and $MF_1$ make $MF_1$ a more attractive subject of study.

## MATERIALS AND METHODS

### Enzyme preparation, nucleotide content, and activity essays

$MF_1$ was prepared according to the method of Knowles and Penefsky (1972). The purified enzyme was then treated as described by Edel et al. (1992) to obtain $MF_1$ with three tightly bound nucleotides. This preparation was stored at −80°C as a 15 mg/ml solution in a buffer containing 50 mM HEPES-NaOH (pH 7.0), 2 mM EDTA buffer, and 20% glycerol. The protein concentration was determined by the Bio-Rad protein assay. For calculations, a relative molecular mass of 370,000 Da was used for $MF_1$. Samples with different nucleotide content were prepared by the addition of concentrated protein aliquots to a solution containing the desired amount of nucleotide/$Mg^{2+}$ in the same buffer, and incubated for 1 h at room temperature to ensure equilibration. Nucleotide-depleted $MF_1$ was obtained as described (Garret and Penefsky, 1975), using a 12-cm Sephadex G-50 column in 100 mM Tris-$SO_4$ buffer (pH 7.0) containing 4 mM EDTA and 64% (w/v) glycerol. After elution the protein was concentrated by ultrafiltration and diluted with a sufficient amount of 50 mM HEPES-NaOH buffer (pH 7.0) to obtain a final glycerol concentration of 20% (w/v).

The ATP concentration was measured with the luciferin-luciferase luminiscence assay in a BioOrbit 1250-Luminometer. The ADP concentration was measured after phosphorylation to ATP by pyruvate kinase, using phosphoenol pyruvate as phosphate donor. Each sample was separated in two aliquots for nucleotide determination. In the first one, the free nucleotide content was measured after separation of $MF_1$ from medium nucleotides by ultrafiltration on polysulfone membranes (Millipore Ultrafree-MC). In the second one, total nucleotide content was measured by adding an equal volume of 4% trichloracetic acid to extract bound nucleotides from $MF_1$. Finally, bound nucleotides were determined by subtracting free nucleotide from the total nucleotide content. When a large excess of nucleotide was employed, free and loosely bound nucleotides were removed by centrifuge elution through 1-ml syringe columns of Sephadex G-50 (Cross and Nalin, 1982).

The hydrolytic ATPase activity was measured spectrophotometrically at 30°C in 50 mM HEPES-KOH (pH 8.0), 5 mM $Mg^{2+}$, and 20% glycerol, using an ATP-regenerating system in which ADP production was detected by measuring NADH oxidation at 340 nm (Edel et al., 1992). Small aliquots were heated in closed plastic containers, placed in a water bath, and heated at a constant rate of 19°C/h, or kept at a constant temperature. When the desired temperature or time was reached, the aliquot was quickly cooled to 30°C and assayed for ATPase activity.

### Differential scanning calorimetry

DSC measurements were carried out on a MicroCal MC-2+ microcalorimeter (MicroCal, Northampton, MA). Data were processed with the Origin software. $MF_1$ samples were introduced into the chamber cell at a final concentration of 1.0 mg/ml in the same HEPES buffer as used for storage and containing the desired amount of nucleotides: ATP, ADP, or AMPPNP (Sigma, Madrid, Spain) and $Mg^{2+}$. The same medium was placed in the reference cell. The heating rate was 19°C/h, unless otherwise stated, and data were collected from 25°C to 80°C. After the first scan each sample was cooled back to 25°C and reheated in the same conditions to check reversibility. All of the thermal transitions were found to be irreversible; therefore the thermograms corresponding to the reheating scans were taken as instrumental baselines and subtracted from the first scan. Chemical baselines were constructed and subtracted as described by Takahashi and Sturtevant (1981) to obtain the excess heat capacity ($C_p^{ex}$) of transition. If necessary, data were smoothed by adjacent point average. A second-order polynomial was fitted to the 10% top of the calorimetric trace, and the maximum of the fitted polynomial was taken as the transition temperature ($T_m$) and the maximum excess heat capacity ($C_p^{max}$). The calorimetric enthalpy ($\Delta H$) was calculated by numeric integration over the transition and normalization of the $MF_1$ concentration. The calorimetric traces were analyzed as described (Sánchez-Ruiz et al., 1988; Galisteo et al., 1992; Sánchez-Ruiz, 1992).

To rule out the possibility that the effects of millimolar concentrations of nucleotides and $Mg^{2+}$ on the calorimetric profile could be a consequence of an increase in ionic strength, some controls were carried out. The presence of 40 mM NaCl or 13 mM $Na_2SO_4$, which gave an ionic strength comparable to the highest concentrations of nucleotides or $Mg^{2+}$ examined (5 mM), did not modify the temperature of $MF_1$ denaturation. Therefore, it

can be concluded that the changes observed in the presence of nucleotides were not caused by an increase in ionic strength but by specific binding.

### Fluorescence measurements

$MF_1$ (1 mg/ml) was preincubated for 10 min at 25°C with the indicated concentration of 2′(3′)-o-(trinitrophenyl)adenosine-5′-triphosphate (TNPATP) (Molecular Probes, Eugene, OR) in the same buffer used for DSC experiments. Fluorescence measurements were carried out in an SLM-Aminco spectrofluorimeter. The cuvette holder was thermostatted, and the temperature was increased at a constant rate of 50°C/h, higher than that used in DSC experiments, to minimize the degradation of the probe. Excitation was at 410 nm, and emission was recorded between 440 and 700 nm. Control experiments were carried out in the absence of $MF_1$ with the same concentration of TNPATP in the cuvette, to subtract the contribution of free TNPATP to the measured fluorescence.

## RESULTS AND DISCUSSION

### Thermal denaturation of purified $MF_1$

The purified $MF_1$, diluted to 1 mg/ml in EDTA and glycerol buffer, contained three endogenous, tightly bound nucleotides (two ADP and one ATP), in agreement with earlier data (Edel et al., 1992). Fig. 1 *A* shows a calorimetric profile of such a sample together with a second scan taken afterward. A broad and asymmetrical endothermic transition is observed with a maximum at 55°C and a denaturation enthalpy value of 5400 kJ $mol^{-1}$. The thermal unfolding is irreversible, because the reheating scan shows no endotherm. The transition temperature coincides with the midpoint of unfolding visualized by infrared spectroscopy (Cladera et al., 1995). As expected, an irreversible loss of ATPase activity was observed over the same temperature range as the calorimetric transition (Fig. 1 *B*). The loss of enzymatic activity implies, at least, denaturation of the catalytic binding sites or the loss of intersubunit cooperativity needed for catalysis. To correlate the loss of activity with the release of endogenous nucleotides, bound nucleotides were measured as a function of temperature. As shown in Fig. 1 *C*, all three endogenous nucleotides are released with a midpoint of 55°C, again matching the calorimetric transition. Because two of the endogenous nucleotides are bound at noncatalytic sites (Kironde and Cross, 1986; Edel et al., 1992), it can be concluded that both catalytic and noncatalytic binding domains lose their structure irreversibly at the temperature range of the calorimetric transition.

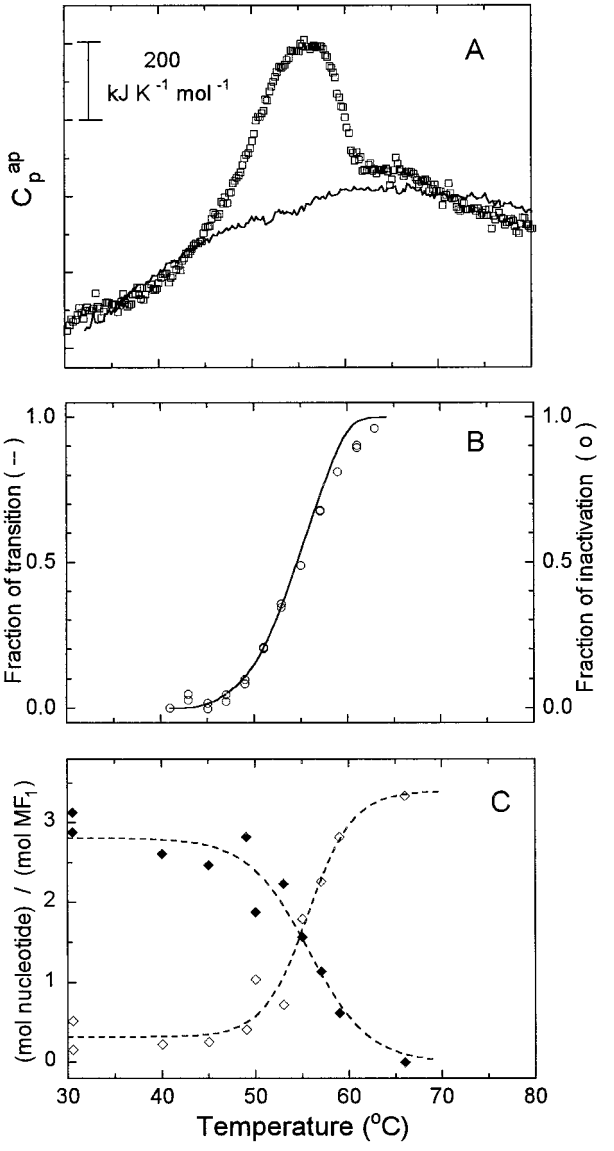


FIGURE 1 Thermal denaturation of purified $MF_1$. $MF_1$ was dissolved at 1.0 mg/ml in HEPES-NaOH 50 mM (pH 7.0) buffer, containing 2 mM EDTA and 20% (w/v) glycerol (EDTA-buffer). The heating rate was 19°C/h. (*A*) □, First DSC scan at 19°C/h. ——, Reheating DSC scan. (*B*) ○, Fraction of irreversible loss of ATPase activity as a function of temperature. ——, Fraction of calorimetric transition, as fraction of enthalpy. (*C*) Release of endogenously bound nucleotides as a function of temperature, during heating scan. ◆, Nucleotide bound to $MF_1$. ◇. Free nucleotide. ——, Best fitting of sigmoidal function, with midpoints at 56 ± 1.5°C, and 55 ± 1.5°C, respectively.

### Kinetic analysis for the thermal denaturation of $MF_1$

Because the thermal denaturation is completely irreversible, no thermodynamic information can be obtained from the DSC trace. A kinetic approach, however, can reveal useful information on the denaturation process (Sánchez-Ruiz, 1992, 1995; Lepock et al., 1992). The kinetics of inactivation of $MF_1$ were studied by monitoring the loss of ATPase activity at different temperatures in the range of the DSC transition (Fig. 2). Analysis of the decay curves in Fig. 2 indicates that the ATPase activity does not decay as a single exponential, but can be well fitted with two overlapping exponentials. This kind of decay implies the existence of at least one significantly populated intermediate state between the native and the final irreversible state (Arriaga et al., 1992). We used a simple three-state model:

$$N \underset{k_2}{\overset{k_1}{\rightleftarrows}} U \xrightarrow{k_3} F \qquad (1)$$

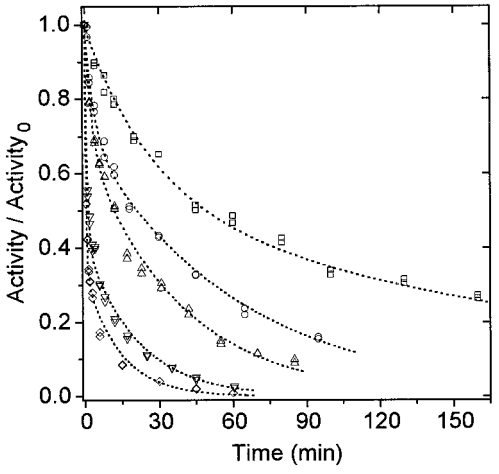


FIGURE 2 Kinetics of inactivation of purified $MF_1$. Samples of $MF_1$ in the same conditions as in Fig. 1 were incubated for the indicated time periods, at 50.0°C (□), 53.0°C (○), 55.0°C (△), 58.0°C, (▽), and 60.0°C (◇). After cooling, the remaining ATPase activity at 30°C was measured and normalized relative to the activity measured without heating (zero time). – – –, Best fits to the kinetic three-state model depicted in Eq. 1. The fitted parameters are listed in Table 1.

where the formation of a reversible intermediate (U) precedes the irreversible step to the final state (F). Using the corresponding differential equations (Lepock et al., 1992), the decay of the native state can be easily simulated. Finding the appropriate values for the kinetic constants $k_1$, $k_2$, and $k_3$, the theoretical decay can be reasonably fitted to the experimental data (Fig. 2 and Table 1). Two observations can be made about these values. First, the ratio $k_1/k_2$ (e.g., the equilibrium constant of the first step) is close to unity. Second, the rate of the irreversible step, $k_3$, is only 2–10 times slower than $k_1$ or $k_2$. Both observations indicate that approximations used to analyze thermal denaturation as an apparent two-state kinetic process (Lepock et al., 1992; Sánchez-Ruiz, 1992) are not valid for native $MF_1$. Finally, because $k_2$ is very slow (half-life > 30 min below 50°C) in comparison with the few seconds required for cooling the sample in the inactivation experiments, little recovery of the native enzyme is expected from the intermediate reversible state upon cooling. As a consequence, the irreversible loss of activity and the calorimetric transition should overlap, as they do in our experiments. The precise nature of the intermediate form accumulated during the denaturation process cannot be determined from these experiments only, but at least it should be a catalytically inactive form. The reversible intermediates are usually considered as partially or fully unfolded states (Freire et al., 1990; Sánchez-Ruiz, 1992, 1995).

**TABLE 1 Values of the kinetic constants calculated to fit the three-state model depicted in Eq. 1 to the experimental data of activity decay at each temperature**

| | $MF_1$ containing three endogenous nucleotides | | | Nucleotide-depleted $MF_1$ | | |
|---|---|---|---|---|---|---|
| Temperature (°C) | $k_1$ ($min^{-1}$) | $k_2$ ($min^{-1}$) | $k_3$ ($min^{-1}$) | $k_1$ ($min^{-1}$) | $k_2$ ($min^{-1}$) | $k_3$ ($min^{-1}$) |
| 50 | 0.023 | 0.025 | 0.015 | 0.035 | 0.052 | 0.046 |
| 53 | 0.073 | 0.10 | 0.044 | 0.120 | 0.072 | 0.067 |
| 55 | 0.117 | 0.128 | 0.060 | — | — | — |
| 56 | — | — | — | 0.41 | 0.126 | 0.105 |
| 58 | 0.65 | 0.40 | 0.082 | 0.79 | 0.129 | 0.114 |
| 60 | 1.47 | 0.72 | 0.14 | — | — | — |

## Thermal denaturation of nucleotide-depleted $MF_1$

To determine the role of the endogenous nucleotides on the thermal stability of $MF_1$, the thermal denaturation of $MF_1$ depleted of nucleotides (nd-$MF_1$) was studied. Denaturation of nd-$MF_1$ diluted in the same buffer as native $MF_1$ occurs at $T_m$ = 53°C, ~2° lower than $MF_1$. The enthalpy of the transition determined from the calorimetric trace is 4600 kJ $mol^{-1}$ (Fig. 3, *trace a*). Thus the three endogenous nucleotides play a minor stabilizing role, because the effect of removing them from $MF_1$ caused only a small decrease in both enthalpy and $T_m$.

The kinetics of inactivation of nd-$MF_1$ was similar to that of $MF_1$ and was fitted to a three-state kinetic process (Table 1). The main difference resides in $k_2$, which is clearly lower at high temperature for the nucleotide-depleted enzyme. As a result, the equilibrium is shifted, favoring the intermediate state. This is evidenced as a destabilizing effect observed upon the removal of the endogenous nucleotides.

## Effect of nucleotide binding to exchangeable sites on the thermal denaturation of $MF_1$ in the absence of $Mg^{2+}$

Addition of adenine nucleotides to $MF_1$ containing the three endogenous tightly bound nucleotides caused notable

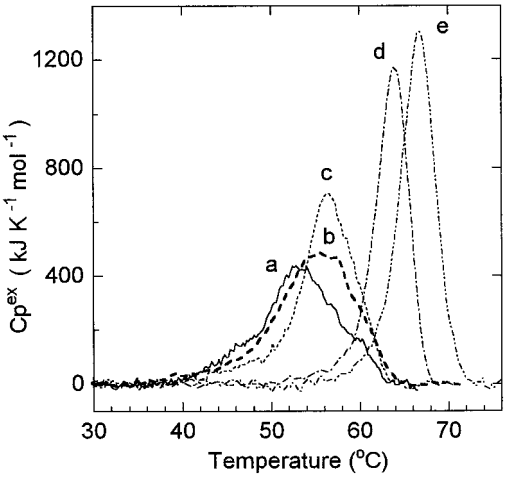


FIGURE 3 Nucleotide effect on the thermal denaturation of $MF_1$ in the absence of $Mg^{2+}$. Experimental conditions were as in Fig. 1. Calorimetric traces are given after subtraction of the instrumental baseline; the correction for the chemical baseline was almost negligible. (*a*) Nucleotide-depleted $MF_1$. (*b*) Purified $MF_1$. (*c*) $MF_1$ in the presence of 40 μM ADP. (*d*) $MF_1$ in the presence of 5 mM ADP. (*e*) $MF_1$ in the presence of 5 mM ATP. The parameters obtained from these transitions are listed in Table 2.

changes in the DSC profiles. Table 2 displays the main parameters of the calorimetric transition recorded after incubation with different nucleotide concentrations. At low concentrations, 10–50 $\mu$M, the thermal transition became narrower, but without any significant change in enthalpy or $T_m$ (see Fig. 3, *trace c*). In this range of concentrations we found four or five nucleotides bound to $MF_1$. These extra one or two nucleotides bound to the starting $MF_1$ are not tightly bound, however, because they were removed during Sephadex column centrifugation. Thus the sites filled in the micromolar range of nucleotide concentration are easily (fast) exchanged with the medium.

In contrast, the presence of adenine nucleotides in the millimolar range noticeably shifted the $T_m$ to higher temperatures with a further narrowing of the transition. Incubation with 5 mM ADP increased both $T_m$ to 64°C and $\Delta H$ to 5800 kJ mol$^{-1}$, whereas incubation with 5 mM ATP increased $T_m$ to 66.8°C and $\Delta H$ to 6800 kJ mol$^{-1}$ (Fig. 3, *traces d* and *e*). At this high nucleotide concentration, all of the nucleotide binding sites are probably filled, but only tightly bound nucleotides could be accurately determined after separation from the nucleotide excess. Incubation with 5 mM ADP did not modify the amount of tightly bound nucleotides present in the starting $MF_1$ preparation, whereas incubation with 5 mM ATP resulted in three ATPs and one ADP being tightly bound. So only ATP significantly increased the total amount of tightly bound nucleotide, displacing one of the originally bound ADP molecules as well, most likely the ADP at the tight catalytic site.

**TABLE 2 Calorimetric parameters for the thermal denaturation of $MF_1$ under different nucleotide or $Mg^{2+}$ content**

| Added nucleotide or $Mg^{2+}$ | Total nucleotide (mM) | $T_m$ (°C) | $\Delta H^{cal}$ (kJ mol$^{-1}$) | $E_a$* (kJ mol$^{-1}$) |
|---|---|---|---|---|
| —[#] | $\sim 10^{-3}$ | 52.8 | 4600 | — |
| —[§] | $7\ 10^{-3}$ | 55.2 | 5400 | — |
| ADP | $1.5\ 10^{-2}$ | 55.4 | 5600 | 220 |
| ADP | $5.0\ 10^{-2}$ | 55.5 | 5500 | 320 |
| ADP | 2.0 | 62.4 | 5400 | 550 |
| ADP | 5.0 | 64.0 | 5800 | 580 |
| ATP | 0.3 | 62.2 | 5200 | 540 |
| ATP | 2.0 | 66.5 | 5600 | 490 |
| ATP | 5.0 | 66.8 | 6800 | 520 |
| $Mg^{2+}$ | $7\ 10^{-3}$ | 59.5 | 6100 | — |
| ADP · $Mg^{2+}$ | 5.0 | 61.9 | $\sim$4000 | — |
| ATP · $Mg^{2+}$ | 0.3 | 62.7 | $\sim$5000 | — |
| ATP · $Mg^{2+}$ | 5.0 | 62.5 | $\sim$6000 | — |
| AMPPNP · $Mg^{2+}$[¶] | 0.25 | 68.4 | 6600 | 700 |
| AMPPNP · $Mg^{2+}$ | 5.0 | 70.1 | 6000 | 720 |

Experimental conditions were as in Fig. 1. Samples containing $Mg^{2+}$ were supplemented with 7 mM $MgCl_2$.

*Activation energy of denaturation process calculated from the calorimetric trace, using an apparent two-state model (see Eq. 2).

[#]Nucleotide-depleted $MF_1$.

[§]Purified $MF_1$ containing three endogenous nucleotides.

[¶]The incubation media also contained 3 mM sodium azide and 5 $\mu$M ADP.

This general pattern of thermal stabilization upon nucleotide binding is in agreement with previous studies on $MF_1$ (Cladera et al., 1995), $CF_1$ (Wang et al., 1993), and the whole enzyme $TF_0F_1$ from the thermophylic *Bacillus* PS3 (Villaverde et al., 1997) or $CF_0F_1$ from spinach chloroplast (unpublished observations). The more nucleotides are bound at the interfaces between the $\alpha$ and $\beta$ subunits, the more additional stabilization is provided to the complex, at least through hydrogen bonding and hydrophobic contacts.

Because a direct determination of loosely bound nucleotides is not possible in the presence of a large excess of nucleotides, the fluorescent derivative TNPATP was used to monitor its release from these sites upon heating. This ATP analog binds to the vacant catalytic sites of $MF_1$ with a sevenfold increase in fluorescence emission, and in contrast to ATP, TNPATP binds to these sites with high affinity (Grubmeyer and Penefsky, 1981; Murataliev and Boyer, 1994). A sample of $MF_1$ with 2 mol of bound TNPATP/mol $MF_1$ was heated at a constant rate, and its fluorescence was continuously measured. A sharp drop in fluorescence was observed with a midpoint at 61°C (see Fig. 4), caused by the release of TNPATP due to denaturation of the TNPATP binding sites (i.e., catalytic sites for ATP). Cooling the sample did not restore the initial value of fluorescence, which remained similar to that of free TNPATP. An aliquot of the same sample was analyzed by DSC; the fraction of the calorimetric transition is shown in Fig. 4. There is an excellent agreement between the calorimetric transition and the unbinding of TNPATP. It can be concluded that tight and loose nucleotide binding sites lose their native structure over the same temperature range.

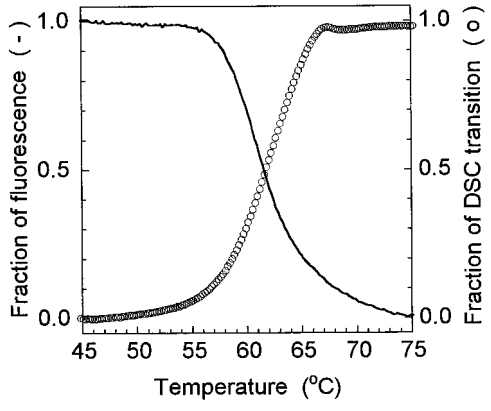


FIGURE 4 Release of tightly bound TNPATP from $MF_1$. $MF_1$ was dissolved at 0.9 mg/ml in EDTA buffer and fluorimetrically titrated with TNPATP until 2 mol of TNPATP/mol $MF_1$ was bound to the protein. (Total TNPATP equals 8.1 $\mu$M.) One aliquot has been scanned at 50°C/h in the DSC, and a second one was heated at the same rate, and its fluorescence emission at $\lambda_{max}$ was continuously collected. ——, Net irreversible change in fluorescence of bound TNPATP. ○, Fraction of the calorimetric transition expressed as a fraction of enthalpy.

### Kinetic analysis of the thermal denaturation of $MF_1$ in the presence of excess nucleotides

The kinetics of inactivation of $MF_1$ were also measured in the presence of 5 mM ATP. They can be fitted to a single exponential decay. Fig. 5 *A* shows the loss of activity versus time, for $MF_1$ samples in 5 mM ATP at five different temperatures. From the slopes of the linear regression curves, the kinetic constant of inactivation was determined at each temperature. The inset in Fig. 5 *A* shows the Arrhenius plot of the data, which gives an activation energy ($E_a$) of 420 ± 15 kJ mol$^{-1}$ for the thermal inactivation process.

The single exponential kinetics of inactivation suggest that a two-state kinetic model (Sánchez-Ruiz et al., 1988; Sánchez-Ruiz, 1995) is sufficient to analyze the calorimetric profiles observed for $MF_1$ in 5 mM ATP following the equation

$$N \xrightarrow{k} F$$

Mathematical elaboration (Galisteo et al., 1992; Sánchez-Ruiz et al., 1988; Sánchez-Ruiz, 1995) leads to an algebraic expression that describes the calorimetric profile as a function of three parameters, $T_m$, $C_p^{max}$, and $E_a$. Fig. 5 *B* shows the fitting of the experimental DSC points to this equation, which gives an $E_a$ value of 510 ± 20 kJ mol$^{-1}$. Three other independent expressions (see Sánchez-Ruiz et al., 1988) allow us to estimate $E_a$, and an average value of 530 ± 20 kJ mol$^{-1}$ was found. This value deviates by ~20% from the value calculated from the kinetics of inactivation (420 ± 15 kJ mol$^{-1}$). Moreover, the $E_a$ calculated from the effect of the heating rate on the $T_m$ gave an $E_a$ of 430 ± 20 kJ mol$^{-1}$.

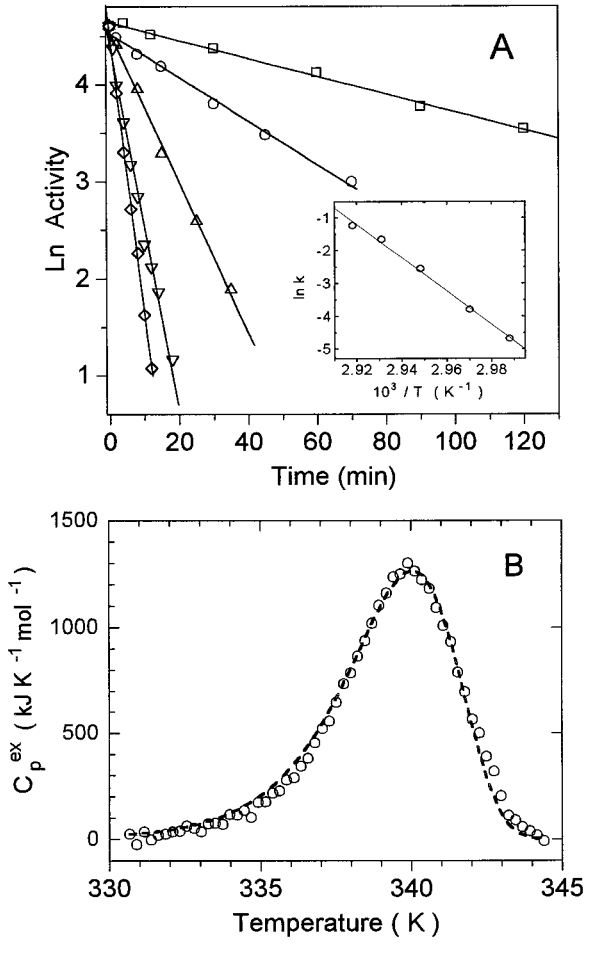


FIGURE 5 Two-state kinetic model of the thermal denaturation of $MF_1$ in EDTA-5 mM ATP. Samples were prepared as in Fig. 1, but with 5 mM ATP added. (*A*) Kinetics of inactivation. Samples were heated during the indicated times at 61.5°C (□), 63.5°C (○), 66.0°C (△), 68.0°C (▽), and 69.5°C (◇). After cooling, the remaining ATPase activity at 30°C was measured. ——, Linear fittings to first-order kinetics: ln(Activity) = $-kt$. *Inset*: Arrhenius plot of the kinetic constants. (*B*) Nonlinear least-squares fit of the DSC trace, to the equation predicted by the two-state kinetic model. ○, Experimental excess heat capacity; ——, calculated best fitting ($C_p^{max}$ = 1260 kJ K$^{-1}$ mol$^{-1}$, $T_m$ = 340.2 K, $E_a$ = 510 kJ mol$^{-1}$).

Hence it seems that a two-state kinetic model, although valid as a first approximation, is a too simple approach to describe the thermal denaturation process of $MF_1$, a complex multimeric enzyme, containing nine subunits and six nucleotide binding sites. A way to deal with the irreversible denaturation of complex protein systems was developed by Sánchez-Ruiz (1992), based on the three-state model depicted in Eq. 1, and assuming that ligand binding or dissociation into subunits is included in the first equilibrium step. In case the equilibrium step is fast and strongly shifted to the folded state, quantitative relationships between protein or nucleotide concentration effects on the $T_m$ can be deduced from this model. However, if the irreversible step is very fast, the folding equilibrium will not be stablished, and no effects of protein or nucleotide concentration on the $T_m$ will be observed. An experimental confirmation of the existence of protein or nucleotide concentration effects on the $T_m$ would suggest that either monomerization of subunits or nucleotide equilibrium exists as a step previous to denaturation.

A protein concentration effect on the temperature of inactivation was hardly observed for $MF_1$ in 5 mM ATP, because a 100-fold dilution lowered the $T_m$ by only 1°C. Considering $MF_1$ as a hexamer ($\alpha_3\beta_3$), the model described by Sánchez-Ruiz (1992) would predict a decrease in $T_m$ of 7°C. Thus it can be concluded that in the presence of excess nucleotide, no dissociation equilibrium into subunits is established before denaturation.

The effect of nucleotide-binding equilibrium on $T_m$ is plotted in Fig. 6. According to Sánchez-Ruiz (1992), and assuming that no dissociation equilibrium into subunits occurs, the slope of this plot is $-E_a/(R\nu)$, where $\nu$ is the number of ligand binding sites in equilibrium. From the value of $E_a$ obtained at 5 mM nucleotide, $\nu$ was estimated as 0.85 ± 0.15 for ATP and 1.0 ± 0.2 for ADP. In both cases a value close to one binding site in equilibrium was obtained, suggesting that the notable stabilizing effect (increase in $T_m$) observed at 5 mM nucleotide can be attributed to the shift of the equilibrium from an $MF_1$ form filled with five nucleotides to a form fully loaded with six nucleotides.

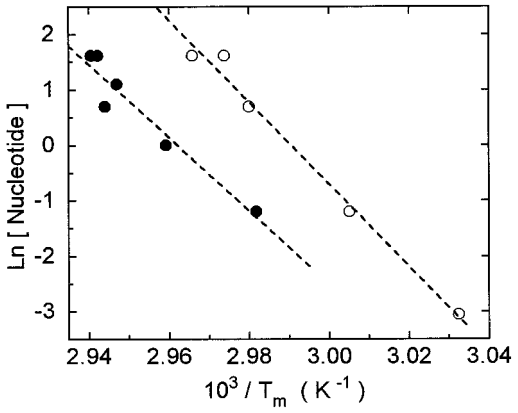


FIGURE 6 Effect of nucleotide concentration on the $T_m$ of denaturation of $MF_1$ incubated with ADP (○) or ATP (●). – – –, Least-squares linear fits to the data points. Experimental conditions as in Fig. 1.

Comparing this result with the more complex decay observed for $MF_1$ without added nucleotides (Fig. 2), it can be concluded that high concentrations of nucleotides modify the kinetic constants, giving rise to an apparent single exponential kinetics of inactivation, thus stabilizing the enzyme. It is tempting to speculate that the large stabilizing effect at high nucleotide concentrations is related to binding at the low-affinity noncatalytic site (Jault and Allison, 1993; Edel et al., 1993).

## Effect of nucleotide binding on the thermal denaturation of $MF_1$ in the presence of $Mg^{2+}$

The effect of $Mg^{2+}$ and nucleotide plus $Mg^{2+}$ on the thermal denaturation of $MF_1$ was also analyzed. The amount of tightly bound nucleotides was measured. Incubation with 5 mM ADP-$Mg^{2+}$ increased the amount of tightly bound nucleotides only slightly to a total of 3.5 mol/mol $MF_1$, whereas 5 mM ATP-$Mg^{2+}$ increased the tightly bound nucleotides to a total of 4.5 mol/mol $MF_1$. The kinetic analysis of the denaturation process of $MF_1$ in the presence of excess nucleotide plus $Mg^{2+}$ closely correlated with an apparent two-state process, similar to the situation found in the presence of nucleotides without $Mg^{2+}$. The Arrhenius plot of the kinetic denaturation constants yielded an activation energy for denaturation of 320 ± 25 kJ $mol^{-1}$.

The calorimetric profiles recorded for $MF_1$ samples exposed to $Mg^{2+}$, ATP · $Mg^{2+}$, or ADP · $Mg^{2+}$ are shown in Fig. 7 (*traces a, b,* and *c*), and the corresponding parameters are listed in Table 2. Addition of $Mg^{2+}$ to $MF_1$ samples caused a remarkable increase in $T_m$ from 55.2°C to 59.5°C, whereas subsequent addition of nucleotides only caused a small stabilizing effect ($T_m \approx 62$°C). The DSC thermograms of the nucleotide · $Mg^{2+}$ · $MF_1$ samples (*traces b* and *c*) show a large difference in heat capacity before and after denaturation, which arises from comparatively low $C_p$ values of the enzyme at low temperatures. However, this $\Delta C_p$ was not detected in the $MF_1$ samples containing only $Mg^{2+}$ or nucleotides. The main functional difference due to

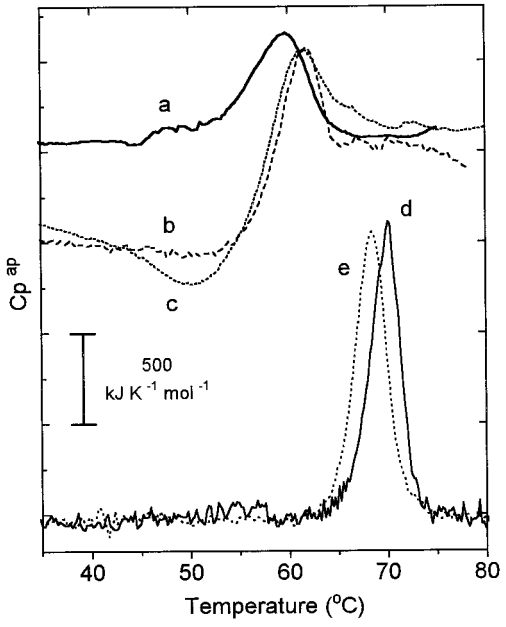


FIGURE 7 Thermal denaturation of $MF_1$ in the presence of $Mg^{2+}$ and $Mg^{2+}$ · nucleotides. Conditions are the same as in Fig. 1, but with 7 mM $MgCl_2$. The DSC scans correspond to $MF_1$ in $Mg^{2+}$ buffer with (*a*) no nucleotide; (*b*) 5 mM ATP; (*c*) 5 mM ADP; (*d*) 5 mM AMPPNP; and (*e*) 0.25 mM AMPPNP, 5 μM ADP, 3 mM $NaN_3$. Traces *d* and *e* are corrected for instrumental baselines and displaced on the *y* axis for clarity. The parameters measured from these transitions are listed in Table 2.

$Mg^{2+}$ is that in its presence the enzyme is hydrolytically active. After ATP hydrolysis, or simply by incubation with ADP · $Mg^{2+}$, $MF_1$ shifts to an ADP- and $Mg^{2+}$-dependent inhibited state, which contains tightly bound ADP at a catalytic site (Murataliev, 1992). The presence of an inhibited state in the ADP · $Mg^{2+}$- and ATP · $Mg^{2+}$-$MF_1$ samples was confirmed by the measurement of a slow rate of ATP hydrolysis during the first 1–2 min after dilution of the preparation in the regenerating system used for activity measurements. Thus both findings, the large $\Delta C_p$ and the small stabilizing effect of nucleotides plus $Mg^{2+}$, can be attributed to the formation of this inhibited state.

A way to study the effect of nucleotide · $Mg^{2+}$ binding on the stability of $MF_1$, avoiding catalysis and subsequent formation of the ADP · $Mg^{2+}$ inhibited state, is to use the nonhydrolyzable analog AMPPNP. Fig. 7 (*trace d*) shows the thermogram obtained from a $MF_1$ sample incubated with 5 mM AMPPNP · $Mg^{2+}$. This trace did not show any significant difference in $C_p$ between the native and the denatured states. Moreover, this sample is remarkably stable: $T_m$ is 70.1°C (see Table 2). The effect of AMPPNP · $Mg^{2+}$ on $MF_1$ stability, then, resembles the effect of ATP in the absence of $Mg^{2+}$.

Abrahams et al. (1994) suggested that the structure of $MF_1$ crystallized in the presence of 250 μM AMPPNP and azide could be that of the ADP-inhibited form. Fig. 7 (*trace e*; see also Table 2) shows the calorimetric trace of a $MF_1$ sample incubated under the same conditions as used by Abrahams et al. (1994) for crystallization (buffer containing

AMPPNP 0.25 mM, ADP 5 $\mu$M, sodium azide and $Mg^{2+}$). This sample shows again a transition without any increase in $C_p$ between the native and the denatured state. The $T_m$ is lower than in trace c, probably because one nucleotide binding site is still empty after incubation with 0.25 mM AMPPNP, whereas all of the nucleotide binding sites are filled in the presence of 5 mM nucleotide (Senior et al., 1995; Löbau et al. 1997). This result suggests that the $MF_1$ structure crystallized in the presence of AMPPNP · $Mg^{2+}$ is not exactly the same as that of the ADP · $Mg^{2+}$-inhibited state formed under functional conditions for the enzyme.

## CONCLUSION

The general trend observed in this work is the stabilizing effect of nucleotide binding on the thermal stability of $MF_1$. The three endogenous, tightly bound nucleotides stabilize the enzyme only slightly as compared with the nucleotide-depleted enzyme. Both forms of $MF_1$ denature with accumulation of one reversible intermediate state. In the absence of any nucleotide, the equilibrium favors the unfolded form.

The presence of nucleotide in excess, either in the presence or in the absence of $Mg^{2+}$, prevents the accumulation of significant amounts of unfolded intermediates during denaturation, and the process can be described on the basis of apparent two-state kinetics. The addition of nucleotide in the absence of $Mg^{2+}$ results in a sharp calorimetric transition, with a marked increase in $T_m$. This effect is due to the binding of one nucleotide to a specific site of $MF_1$ in fast equilibrium with the free ligand.

In the presence of $Mg^{2+}$ the stabilizing effect induced by nucleotides is smaller and the calorimetric transition is superimposed on a large change in heat capacity. These differences suggest that the enzyme states are significantly different in the presence or absence of $Mg^{2+}$. From the functional point of view, the presence of nucleotide and $Mg^{2+}$ brings the enzyme into an inhibited state (Murataliev, 1992; Milgrom and Cross, 1993; Jault and Allison, 1993; Jault and Allison, 1994). Moreover, the presence of $Mg^{2+}$ strongly modifies the catalytic sites, equivalent affinities for nucleotides being replaced by different affinities for nucleotide at each site (Senior et al. 1995, Weber and Senior, 1996). The presence of different affinities for nucleotide of each catalytic site is in agreement with the binding change mechanism of catalysis (Boyer, 1993), which minimally requires one tight site (high affinity for ATP) and one loose site with low affinity.

On the other hand, when the nonhydrolyzable analog AMPPNP is used, the DSC transitions resemble those obtained with ATP in the absence of $Mg^{2+}$. This finding indicates that, when binding sites are filled with nucleotides but the enzyme is blocked (stopped), either by the presence of a nonhydrolyzable analogue or by the absence of $Mg^{2+}$, this binding results in a more stable form of the enzyme than that of the ADP · $Mg^{2+}$ inhibited state.

Our results give support to the concept pointed out by Löbau et al. (1997) that the structure crystallized in the presence of AMPPNP · $Mg^{2+}$ could correspond to an intermediate state in the catalytic cycle, rather than the ADP · $Mg^{2+}$ inhibited state, as originally suggested by Abrahams et al. (1994).

Finally, it is noticeable that the two incubation media we found to yield the most stable states of $MF_1$ (ATP in the absence of $Mg^{2+}$ and AMPPNP in the presence of $Mg^{2+}$) are the media used in crystallization studies by Pedersen et al. (1995) and Abrahams et al. (1994), respectively. The one state, however, may be considered as a "ready" state, the other as an intermediate state in the catalytic cycle, with consequences for the symmetry of the structure.

We are indebted to Elodia Serrano for technical assistance.

This work was supported by grants from the European Community (Biotechnology, Bio 2 CT-930078), from the Comisión Interministerial de Ciencia y Tecnología (Bio93-1058-CE), and from the Direcció General de Recerca (1995SGR 00481).

## REFERENCES

Abrahams, J. P., A. G. W. Leslie, R. Lutter, and J. E. Walker. 1994. Structure at 2.8 Å of $F_1$-ATPase from bovine heart mitochondria. *Nature.* 370:621–628.

Arriaga, P., M. Menéndez, J. M. Villacorta, and J. Laynez. 1992. Differential scanning calorimetric study of the thermal unfolding of $\beta$-lactamase I from *Bacillus cereus. Biochemistry.* 31:6603–6607.

Berden, J. A., A. F. Hartog, and C. M. Edel. 1991. Hydrolysis of ATPby $F_1$ can be described only on the basis of a dual-site mechanism. *Biochim. Biophys. Acta.* 1057:151–156.

Boyer, P. D. 1993. The binding change mechanism for ATP synthase. Some probabilities and possibilities. *Biochim. Biophys. Acta.* 1140: 215–250.

Cladera, J., J. Villaverde, A. F. Hartog, E. Padrós, J. A. Berden, J.-L. Rigaud, and M. Duñach. 1995. Influence of nucleotides on the structure and on the thermal stability of mitochondrial $F_1$ visualized by infrared spectroscopy. *FEBS Lett.* 371:115–118.

Cross, R. L., C. Grubmeyer, and H. S. Penefsky. 1982. Mechanism of ATP hydrolysis by beef heart mitochondrial ATPase. Rate enhancements resulting from cooperative interactions between multiple catalytic studies. *J. Biol. Chem.* 257:12101–12105.

Cross, R. L., and C. M. Nalin. 1982. Adenine nucleotide binding sites on beef heart $F_1$-ATPase. Evidence for three exchangeable sites that are distinct from three noncatalytic sites. *J. Biol. Chem.* 257:2874–2881.

Edel, C. M., A. F. Hartog, and J. A. Berden. 1992. Inhibition of mitochondrial $F_1$-ATPase activity by binding of (2-azido-)ADP to a slowly exchangeable non-catalytic nucleotide binding site. *Biochim. Biophys. Acta.* 1100:329–338.

Edel, C. M., A. F. Hartog, and J. A. Berden. 1993. Identification of an exchangeable non-catalytic site on mitochondrial $F_1$-ATPase, which induces the negative cooperativity of ATP hydrolysis. *Biochim. Biophys. Acta.* 1142:327–335.

Freire, E., W. W. Osdol, O. L. Mayorga, and J. M. Sánchez-Ruiz. 1990. Calorimetrically determined dynamics of complex unfolding transitions in proteins. *Annu. Rev. Biophys. Chem.* 19:159–188.

Futai, M., H. Omote, and M. Maeda. 1995. *Escherichia coli* $H^+$-ATPase (ATP synthase): catalytic site and roles of subunit interactions in energy coupling. *Biochem. Soc. Trans.* 23:785–789.

Galisteo, M. L., F. Conejero-Lara, J. Núñez, J. M. Sánchez-Ruiz, and P. L. Mateo. 1992. A calorimetric approach to the kinetics of the irreversible thermal denaturation of proteins. *Thermochim. Acta.* 199:147–157.

Garret, N. E., and H. S. Penefsky. 1975. Interaction of adenine nucleotides with multiple binding sites of beef heart mitochondrial adenosine triphosphatase. *J. Biol. Chem.* 250:6640–6647.

Gresser, M. J., J. A. Myers, and P. D. Boyer. 1982. Catalytic site cooperativity of beef heart mitochodrial $F_1$ adenosine triphosphatase. Correlations of initial velocity, bound intermediate, and oxygen exchange measurements with an alternating three-site model. *J. Biol. Chem.* 257: 12030–12038.

Grubmeyer, C., and H. S. Penefsky. 1981. Cooperativity between catalytic sites in the mechanism of action of beef heart mitochondrial adenosine triphosphatase. *J. Biol. Chem.* 256:3728–3734.

Haltia, T., and E. Freire. 1995. Forces and factors that contribute to the structural stability of membrane proteins. *Biochim. Biophys. Acta.* 1241: 295–322.

Jault, J. M., and W. S. Allison. 1993. Slow binding of ATP to noncatalytic nucleotide binding sites which accelerates catalysis is responsible for apparent negative cooperativity exhibited by bovine mitochondrial $F_1$-ATPase. *J. Biol. Chem.* 268:1558–1566.

Jault, J. M., and W. S. Allison. 1994. Hysteretic inhibition of the bovine mitochondrial $F_1$-ATPaseis due to saturation of noncatalytic sites with ADP which blocks activation of the enzyme by ATP. *J. Biol. Chem.* 269:319–325.

Junge, W., H. Lill, and S. Engelbrecht. 1997. ATP synthase: an electrochemical transducer with rotatory mechanics. *Trends Biochem. Sci.* 22:420–423.

Kironde, F. A. S., and R. L. Cross. 1986. Adenine nucleotide-binding sites on beef heart $F_1$-ATPase. Conditions that affect occupancy of catalytic and noncatalytic sites. *J. Biol. Chem.* 261:12544–12549.

Knowles, A. F., and H. S. Penefsky. 1972. The subunit structure of beef heart mitochondrial adenosine triphosphatase. Isolation procedures. *J. Biol. Chem.* 247:6617–6623.

Lepock, J. R., K. P. Ritchie, M. C. Kolios, A. M. Rodahl, K. A. Heinz, and J. Kruuv. 1992. Influence of transition rates and scan rate on kinetic simulations of differential scanning calorimetry profiles of reversible and irreversible protein denaturation. *Biochemistry.* 31:12706–12712.

Löbau, S., J. Weber, and A. E. Senior. 1997. Nucleotide occupancy of $F_1$-ATPase catalytic sites under crystallization conditions. *FEBS Lett.* 404:15–18.

Milgrom, Y. M., and R. L. Cross. 1993. Nucleotide binding sites on beef heart mitochondrial $F_1$-ATPase. Cooperative interactions between sites and specificity of noncatalytic sites. *J. Biol. Chem.* 268:23179–23185.

Murataliev, M. B. 1992. Adenine nucleotide binding at a noncatalytic site of mitochondrial $F_1$-ATPase accelerates a $Mg^{2+}$- and ADP-dependent inactivation during ATP hydrolysis. *Biochemistry.* 31:12885–12892.

Murataliev, M. B., and P. D. Boyer. 1994. Interaction of mitochondrial $F_1$-ATPase with trinitrophenyl derivatives of ATP and ADP. Participation of third catalytic site and role of $Mg^{2+}$ in enzyme inactivation. *J. Biol. Chem.* 269:15431–15439.

Nalin, C. M., and R. L. Cross. 1982. Adenine nucleotide binding sites on beef heart $F_1$-ATPase. Specificity of cooperative interactions between catalytic sites. *J. Biol. Chem.* 257:8055–8060.

Pedersen, P. L., J. Hullihen, M. Bianchet, L. M. Amzel, and M. S. Lebowitz. 1995. Rat Liver ATP synthase. Relationship of the unique substructure of the $F_1$ moiety to its nucleotide binding properties, enzymatic states, and crystalline form. *J. Biol. Chem.* 270:1775–1184.

Reynafarje, B. D., and P. L. Pedersen. 1996. ATP synthase. Conditions under which all catalytic sites of the $F_1$ moiety are kinetically equivalent in hydrolyzing ATP. *J. Biol. Chem.* 271:32546–32550.

Sánchez-Ruiz, J. M. 1992. Theoretical analysis of Lumry-Eyring models in differential scanning calorimetry. *Biophys. J.* 61:921–935.

Sánchez-Ruiz, J. M. 1995. Differential scanning calorimetry of proteins. *In* Subcellular Biochemistry. Proteins: Structure, Function and Engineering, Vol 24. B. B. Biswas and Siddharta Roy, editors. Plenum Press, New York. 133–176.

Sánchez-Ruiz, J. M., J. L. López-Lacomba, M. Cortijo, and P. L. Mateo. 1988. Differential scanning calorimetry of the irreversible thermal denaturation of thermolisin. *Biochemistry.* 27:1648–1652.

Senior, A. E., J. Weber, and M. K. Al-Shawi. 1995. Catalytic mechanism of *Escherichia coli* $F_1$-ATPase. *Biochem. Soc. Trans.* 23:747–752.

Shapiro, A. B., A. H. Huber, and R. E. McCarty. 1991. Four tight nucleotide binding sites of chloroplast coupling factor 1. *J. Biol. Chem.* 266:4194–4200.

Takahashi, K., and J. M. Sturtevant. 1981. Thermal denaturation of *Streptomyces* subtilisin inhibitor, subtilisin BPN′, and the inhibitor-subtilisin complex. *Biochemistry.* 20:6185–6190.

Villaverde, J., J. Cladera, E. Padrós, J.-L. Rigaud, and M. Duñach. 1997. Effect of nucleotides on the thermal stability and on the deuteration kinetics of the thermophilic $F_0F_1$ ATP synthase. *Eur. J. Biochem.* 244: 441–448.

Wang, Z. Y., E. Freire, and R. E. McCarty. 1993. Influence of nucleotide binding site occupancy on the thermal stability of the $F_1$ portion of the chloroplast ATP synthase. *J. Biol. Chem.* 268:20785–20790.

Weber, J., and A. E. Senior. 1996. $F_1F_0$-ATP synthase: development of direct optical probes of the catalytic mechanism. *Biochim. Biophys. Acta.* 1275:101–104.

Weber, J., and A. E. Senior. 1997. Catalytic mechanism of $F_1$-ATPase. *Biochim. Biophys. Acta.* 1319:19–58.